This is the accepted manuscript (postprint) of the following article:
H. Rahmani, E. Salahinejad, *Incorporation of monovalent cations into diopside to improve biomineralization and cytocompatibility*, Ceramics International, 44 (2018) 19200-19206.
https://doi.org/10.1016/j.ceramint.2018.07.140

Incorporation of monovalent cations into diopside to improve biomineralization and cytocompatibility

H. Rahmani, E. Salahinejad*

Faculty of Materials Science and Engineering, K. N. Toosi University of Technology, Tehran, Iran

Abstract

This paper aims to evaluate the structure, bioactivity, biodegradation and cytocompatibility of diopside ($CaMgSi_2O_6$) doped with 2 mol% of Li, Na and K separately substituting for 1 mol% of Mg of diopside. An ethanolic, inorganic-salt coprecipitation method, followed by calcination at 900 °C, was used for synthesis. X-ray diffraction showed that the single-phase diopside structure is kept at this level of substitution; however, the crystallinity and lattice volume of diopside were changed depending on the size difference of the replacement components. According to *in vitro* biological studies, doping of all the alkali ions improves the bioactivity of diopside, with the highest and least effects obtained by K and Na, respectively. The MTT assay of osteoblast-like MG-63 cell cultures indicated that the cell viability and proliferation are improved as a result of using all the dopants, where the most enhancements were found for Na and K. It is eventually concluded that the incorporation of K into diopside ensures the optimal behaviors in terms of bioactivity and biocompatibility *in vitro*.

Keywords: Calcination (A); Spectroscopy (B); Silicate (D); Biomedical applications (E)

* Corresponding Author: Email Address: <salahinejad@kntu.ac.ir>

This is the accepted manuscript (postprint) of the following article:
H. Rahmani, E. Salahinejad, *Incorporation of monovalent cations into diopside to improve biomineralization and cytocompatibility*, Ceramics International, 44 (2018) 19200-19206.
https://doi.org/10.1016/j.ceramint.2018.07.140

1. Introduction

Among bioactive/bioresorbable ceramics, magnesium-containing silicates in the both forms of crystalline and glass are under consideration in biomedicine [1, 2]. Their typical benefit is higher mechanical strength in comparison to apatites and bioglass as the most prevalent bioactive/bioresorbable ceramics. One of the main members of this silicate group is diopside with the composition of $CaMgSi_2O_6$, i.e. a low level of calcium but the high amounts of magnesium and silicon. This particular ionic composition provides significant biocompatibility but limited bioactivity and biodegradation in comparison to the other members of magnesium-containing silicates.

Essentially, there are two approaches to enhancing the bioactivity of bioceramics: nanostructuring and using proper dopants. Pure nanocrystalline/nanoparticulate diopside has been synthesized by several wet-chemical methods like hydrothermal, sol-gel and coprecipitation [3-5]. In this regard, the application of chloride precursors has indicated several advantages, including lowering the formation temperature and the overall synthesis cost of single-phase diopside [6]. Regarding the doping approach, fluoride has been successfully used to control the apatite-formation ability of glassy and crystalline $CaMgSi_2O_6$ (diopside) [7-9]. The presence of the alkali cations of Li^+, Na^+ and K^+ in the body at trace contents creates the idea of their doping in diopside [10]. It would be worth mentioning that these species have been previously employed in other bioceramics, leading to different and occasionally contradictory effects on biological behaviors [11-13].

In this work, with the aim of improving the bioactivity of diopside, Li, Na and K doping was originally conducted by a coprecipitation method using chloride precursors,

This is the accepted manuscript (postprint) of the following article:
H. Rahmani, E. Salahinejad, *Incorporation of monovalent cations into diopside to improve biomineralization and cytocompatibility*, Ceramics International, 44 (2018) 19200-19206.
https://doi.org/10.1016/j.ceramint.2018.07.140

followed by calcination. Afterwards, the obtained structure, bioactivity, biodegradation and cell viability were compared *in vitro*.

2. Experimental procedure

2.1. Sample preparation

Diopside ($CaMgSi_2O_6$) was synthesized through a coprecipitation method using chloride precursors, ethanolic solution and ammonium precipitant, as detailed in Ref. [6]. Lithium (Li), sodium (Na) and potassium (K) was separately doped into diopside as follows. First, $CaCl_2$, $MgCl_2$, and LiCl (NaCl or KCl) at the molar ratio of 1:0.99:0.02 (i.e. 1 mol% of bivalent Mg was replaced with 2 mol% of the monovalent dopants for keeping the charge balance of the product) were added to ethanol under stirring. After complete dissolution, $SiCl_4$ was added at 0 °C and stirred for 30 min. Finally, ammonium hydroxide solution was added to the solution for precipitation. The product was dried at 100 °C for 6 h, grounded and then calcined at 900 °C for 2 h.

2.2. Structural characterization

X-ray diffraction (XRD, CuKα radiation), Fourier transform infrared spectroscopy (FTIR) and field emission scanning electron microscopy (FESEM) were utilized to study the phase, bonding and morphological characteristics of the calcined powders, respectively.

2.3. Bioactivity and biodegradation assessments

In order to compare the bioactivity of the synthesized samples *in vitro*, 0.1 gr of the powders was added to 40 ml of the simulated body fluid (SBF) and kept in an incubator at

This is the accepted manuscript (postprint) of the following article:
H. Rahmani, E. Salahinejad, *Incorporation of monovalent cations into diopside to improve biomineralization and cytocompatibility*, Ceramics International, 44 (2018) 19200-19206.
https://doi.org/10.1016/j.ceramint.2018.07.140

36.5 °C for 7 and 14 days. The immersed samples, after washing and drying, were characterized by FESEM equipped with energy-dispersive X-ray spectroscopy (EDS) and Raman spectroscopy. The exposing SBFs were also analyzed by inductively coupled plasma optical emission spectroscopy (ICP-OES) and pH measurements.

2.4. Cell viability evaluation

For cellular studies. the powder samples were first sterilized in an ethanol solution, washed with phosphate-buffered saline, and then exposed to an UV radiation. Almost 20000 osteoblast-like MG-63 cells were cultured on each sample for 24, 48 and 72 h. The assessment of the cell viability was performed by the MTT assay with three repetitions, in terms of the optical density of viable cells.

3. Results and discussion

3.1. Structural characterizations

Fig. 1 presents the XRD patterns of the calcined powder samples. Single-phase diopside structures ($MgCaSi_2O_6$) were identified in all of the undoped and doped samples by the PANalytical X'Pert HighScore software. Furthermore, the mean crystallite size of diopside was calculated by the Scherrer equation to be about 28.8, 28.5, 27.4 and 27.4 nm for the undoped, Li-doped, Na-doped and K-doped samples, respectively. The minor differences observed in the intensity of the associated XRD peaks in the different samples are related to the difference in the ionic radii and charges of the dopant and magnesium (substitution components). Indeed, the partial substitution of monovalent cations (dopants) for bivalent cations (Mg) breaks the network chains, as follows:

$$O\text{-}Mg\text{-}O \rightarrow O\text{-}D + D\text{-}O \quad (1)$$

This is the accepted manuscript (postprint) of the following article:
H. Rahmani, E. Salahinejad, *Incorporation of monovalent cations into diopside to improve biomineralization and cytocompatibility*, Ceramics International, 44 (2018) 19200-19206.
https://doi.org/10.1016/j.ceramint.2018.07.140

where D represents the monovalent dopants. This consequently gives rise to the reduction in crystallinity [14-18] and XRD peak intensities in comparison to the undoped powder. The contribution of the ionic radius differences is described below in parallel with the network volume variations.

Diopside has a monoclinic structure with the lattice parameters of $a \neq b \neq c$ and the axial angles $\alpha = \gamma = 90 \neq \beta$, where the network volume (V) is equal to "abc sin β". The mentioned crystallographic data were extracted from the diffraction parameters of the most intense XRD peaks, as tabulated in Table 1. According to these results, compared to the undoped sample, the network volume for the sodium- and potassium-doped structures has increased, but it has decreased for the lithium-doped one. Doped ions are essentially located in the vacant lattice sites of the network which are pre-existing or created due to the partial removal of magnesium. As a result, doping distorts the network, depending on the charge and relative size of the substitution components. A larger dopant would distort the lattice, but the replacement of a dopant with an equal or smaller size would be easier. In this study, lithium ions are smaller, potassium ions are larger, and sodium ions are slightly larger (almost equal to) than magnesium ions. Lithium ions tend to react with oxygen existing in the network and to accommodate in the interstitial sites of the silicate network [19]. Nonetheless, sodium and potassium ions are substitutionally replaced with magnesium ions, where the lattice distortion generated by potassium is higher. These facts fairly explains the difference of the network volumes listed in Table 1. Typically, sodium with an ionic radius close to magnesium has led to the least distortion and thereby the closest lattice volume and XRD peak intensity to pure diopside.

This is the accepted manuscript (postprint) of the following article:
H. Rahmani, E. Salahinejad, *Incorporation of monovalent cations into diopside to improve biomineralization and cytocompatibility*, Ceramics International, 44 (2018) 19200-19206.
https://doi.org/10.1016/j.ceramint.2018.07.140

Fig. 2 indicates the FTIR pattern of the synthesized samples after calcination. For all the samples, the peaks around 475 and 517 cm^{-1} are attributed to the O-Mg-O group. Comparatively, these characteristic peaks displays a reduced intensity after doping, as a result of the decrease in the concentration of magnesium which is partially replaced. The peaks of 635 and 675 cm^{-1} belong to O-Si-O; in addition, vibrations at 865, 970 and 1080 cm^{-1} are assigned to the symmetric stretching of Si-O [20]. An additional peak for the Li-doped sample at 1715 cm^{-1} suggests the incorporation of Li ions [21]. Also, vibrations at around 2370 cm^{-1} in the K- and Na-doped samples are attributed to the introduction of the related dopant in the structure [22, 23].

Fig. 3 depicts the FESEM micrograph of the calcined powders. The pure diopside powder particles exhibit irregular shapes with a size of almost 80-800 nm. The Li-doped particles can be categorized into two groups: (i) irregular-shaped particles with a size of about 400-1200 nm and (ii) rod-like particles with the mean smallest dimension of about 70 nm and the mean largest dimension of 500 nm. In comparison to Li, the Na- and K-doping processes result in the domination of the rod-like morphology with a slight increase of the dimensions by 10 nm. Indeed, the introduction of the alkali ions leads to the distortion and breakdown of the silicate chain. This can awhile reduce the consistency and melting point of the ceramics, increase the homologues temperature (T/T_m) applied on the doped samples, and encourage the particle coarsening.

3.2. Bioactivity and biodegradation characterizations

The fixation of a bioactive biomaterial with live tissues in the body is ensured by the formation of an apatite layer on its surface. To compare this characteristic of the synthesized powders, they were exposed to the SBF for various durations. The FESEM micrographs and

This is the accepted manuscript (postprint) of the following article:
H. Rahmani, E. Salahinejad, *Incorporation of monovalent cations into diopside to improve biomineralization and cytocompatibility*, Ceramics International, 44 (2018) 19200-19206.
https://doi.org/10.1016/j.ceramint.2018.07.140

related EDS analyses taken of the samples after 7 days of incubation are presented in Fig. 4. As can be seen, only limited regions of the undoped sample surface are covered by plate-like apatite. However, the Li-doped sample surface uniformly exhibits these plates having a mean thickness of 40 nm and a mean length of 400 nm. For the Na-doped sample, the level of apatite formed is higher than the pure sample, but lower than the Li-doped one. Finally, dense rose-like spherical colonies of about 1.4 μm in diameter are precipitated on the K-doped sample surface. Considering that the synthesized samples are P-free, the related EDS analyses confirm that the precipitates formed after immersion in the SBF are apatite (calcium phosphate). Comparatively, the relative intensity of the P peak in the EDS spectra taken of the different immersed samples is proportional to the amount of apatite formed on them. That is, based on both the FESEM and EDS analyses, the order of the amount of apatite formed on the synthesized samples (bioactivity) is K-doped > Li-doped > Na-doped > undoped.

The Raman spectra of the powder samples after immersion in the SBF are also illustrated in Fig. 5. As well as the characteristic vibrations of the silicate matrices, peaks at 432, 470 and 959 cm^{-1} are related to the symmetric modes of P-O in the PO_4^{3-} functional group. The peak of 602 cm^{-1} is also assigned to the asymmetric vibration of the same group. The 884 cm^{-1} peak is also indicative of C-O in the CO_3^{2-} group [24, 25]. Hence, Raman spectroscopy infers that the precipitates formed on the sample after incubation in the SBF are a kind of hydroxycarbonate apatite, inferring the bioactivity of the synthesized powder samples.

Fig. 6 indicates the ionic composition of the SBF after 7 and 14 days of incubation in contact with the samples. The consumption and thereby decrease of P in the SBF are essentially caused by the formation of apatite on the exposed samples. In this regard, at any given immersion period, a lower concentration means the higher apatite-formation ability of

This is the accepted manuscript (postprint) of the following article:
H. Rahmani, E. Salahinejad, *Incorporation of monovalent cations into diopside to improve biomineralization and cytocompatibility*, Ceramics International, 44 (2018) 19200-19206.
https://doi.org/10.1016/j.ceramint.2018.07.140

the exposed sample. That is, in agreement with the SEM/EDS evaluations, the bioactivity of the synthesized samples ranks as K-doped > Li-doped > Na-doped > undoped. The concentration of Ca^{2+} after 7 days of immersion is increased for all the samples, due to the release of Ca^{2+} from the samples. This reaction is vital for the precipitation of apatite via making the SBF supersaturated with this ion. After 14 days of immersion, the Ca^{2+} concentration is decreased, due to the deposition of Ca^{2+} from the SBF and the formation of apatite on the surfaces. The lower concentration of Ca^{2+} for the Li- and K-doped samples in the 14^{th} day indicates the more precipitation of apatite on their surfaces. The increase in the concentrations of Si and Mg with time also suggests the biodegradation of the samples. The higher rate of calcium degradation than silicon results in the formation of a Si-rich gel-like layer (silanol) on the surface of the samples, which is preferred locations for the nucleation and growth of apatite.

The pH values of the SBFs in contact with the synthesized powders are presented in Fig. 7. For the undoped sample, the increase in pH during the first days is due to the domination of OH^- in the SBF, through the exchange of the cations (Ca^{2+} and Mg^{2+}) existing in the samples and H^+ existing in the SBF. The subsequent decrease is also as a result of the apatite precipitation consuming OH^- of the SBF. This decrease in pH is not observed for the doped samples because the doped ions are gradually released from the samples toward the SBF and exchanged with H^+ of the SBF, even to the 14^{th} day of immersion. In other words, the mentioned cation-exchange reactions buffer the decrease of pH caused by the formation of apatite. Comparatively, the higher pH values of the SBF in contact with the Li- and K-doped samples (i.e. the samples which show the highest bioactivity) over the entire range of the soaking time suggest that the degradation rate plays a critical role in the apatite-formation ability, as detailed below. It is also noteworthy that the pH value of the SBF during

This is the accepted manuscript (postprint) of the following article:
H. Rahmani, E. Salahinejad, *Incorporation of monovalent cations into diopside to improve biomineralization and cytocompatibility*, Ceramics International, 44 (2018) 19200-19206.
https://doi.org/10.1016/j.ceramint.2018.07.140

immersion remains in the range of 7.5 to 8 even in the presence of the dopants, which is beneficial for cytocompatibility.

A number of the multiple ion-exchange reactions, as pointed out above, are responsible for the *in vitro* bioactivity of diopside [26, 27]. Due to the partial replacement of Mg^{2+} with the monovalent dopants (Li^+, Na^+ and K^+), the network chains are distorted and the bridging cations are partially substituted by the non-bridging ones (Eq. 1). This reduces the activation energy of degradation and thus enhances the degradation of the cations existing in the powder structure toward the SBF. Hence, a larger amount of silanol is formed on the surfaces, pH is further increased, and the subsequent formation of calcium phosphate layers is encouraged [28]. The higher level of structural defects introduced by K-doping, as pointed out in the XRD analysis (Fig. 1), explains the higher degradation and thereby bioactivity of this samples, compared with the Li- and Na-doping. The higher bioactivity of the Li-doped samples than the Na-doped one is also attributed to the higher diffusivity level along interstitial sites (preferred locations for Li dopant), as compared to substitutional sites (preferred locations for Na dopant) [29-32].

3.3. Cytocompatibility characterization

The MTT assay was used to quantify the MG-63 cell cultures conducted on the synthesized samples (Fig. 8). As can be seen, for all the culture durations, the cell viability on the undoped sample is not acceptable in comparison to the control; however, doping of all the three alkali ions into diopside has significantly improved cytocompatibility. Typically, the viability on the Na- and K-doped samples is even higher than the control. The increase in the number of viable cells with time is also indicate of cell proliferation. According to the literature, Li ions by mimicking the Wnt signaling pathway advantageously affect cell

This is the accepted manuscript (postprint) of the following article:
H. Rahmani, E. Salahinejad, *Incorporation of monovalent cations into diopside to improve biomineralization and cytocompatibility*, Ceramics International, 44 (2018) 19200-19206.
https://doi.org/10.1016/j.ceramint.2018.07.140

responses [33, 34]. Nonetheless, the mechanism of Na and K effects on biocompatibility is different. By altering the concentration of Na and K in the culture medium, the activity of the sodium-potassium pump is increased. This enhances the activity of adenosine triphosphate receptors, which are responsible for the proliferation of MG-63 cells, in the mitochondria of the cells [35, 36]. The effect of these two ions on pH regulation, as an important factor in cell viability [37], is also noticeable.

4. Conclusions

In this research, the effect of incorporating alkali ions (Li^+, Na^+ and K^+) on the structure, bioactivity, biodegradation and biocompatibility of diopside was studied. The following conclusions were drawn from this work:

1. Depending on the ionic size of the substitution components, the crystallinity and lattice volume of diopside were changed, with the most and least deviations for K and Na, respectively.

2. The application of the dopants altered the *in vitro* bioactivity of diopside in the following ranking: K-doped > Li-doped > Na-doped > undoped.

3. The dopants at the used level (2 % mol) improved the biocompatibility of diopside, where the most beneficial effect was found for Na and K.

4. Considering both the bioactivity and cytocompatibility assessments, K-doping was recognized as the optimal doping species, in comparison to Li and Na.

References

This is the accepted manuscript (postprint) of the following article:
H. Rahmani, E. Salahinejad, *Incorporation of monovalent cations into diopside to improve biomineralization and cytocompatibility*, Ceramics International, 44 (2018) 19200-19206.
https://doi.org/10.1016/j.ceramint.2018.07.140

[1] M. Diba, O.-M. Goudouri, F. Tapia, A.R. Boccaccini, Magnesium-containing bioactive polycrystalline silicate-based ceramics and glass-ceramics for biomedical applications, Current opinion in solid state and materials science, 18 (2014) 147-167.
[2] M. Diba, F. Tapia, A.R. Boccaccini, L.A. Strobel, Magnesium-containing bioactive glasses for biomedical applications, International Journal of Applied Glass Science, 3 (2012) 221-253.
[3] L. Bozadjiev, L. Doncheva, Methods for diopside synthesis, Journal of the University of Chemical Technology and Metallurgy, 41 (2006) 125-128.
[4] S. Hayashi, K. Okada, N. Otsuka, T. Yano, Preparation and characterization of diopside powder by several methods from solution, Journal of materials science letters, 12 (1993) 153-156.
[5] N.Y. Iwata, G.-H. Lee, Y. Tokuoka, N. Kawashima, Sintering behavior and apatite formation of diopside prepared by coprecipitation process, colloids and surfaces B: Biointerfaces, 34 (2004) 239-245.
[6] N. Namvar, E. Salahinejad, A. Saberi, M.J. Baghjeghaz, L. Tayebi, D. Vashaee, Toward reducing the formation temperature of diopside via wet-chemical synthesis routes using chloride precursors, Ceramics International, 43 (2017) 13781-13785.
[7] N. Esmati, T. Khodaei, E. Salahinejad, E. Sharifi, Fluoride doping into SiO 2-MgO-CaO bioactive glass nanoparticles: bioactivity, biodegradation and biocompatibility assessments, Ceramics International, (2018).
[8] M.J. Baghjeghaz, E. Salahinejad, Enhanced sinterability and in vitro bioactivity of diopside through fluoride doping, Ceramics International, 43 (2017) 4680-4686.
[9] E. Salahinejad, M.J. Baghjeghaz, Structure, biomineralization and biodegradation of Ca-Mg oxyfluorosilicates synthesized by inorganic salt coprecipitation, Ceramics International, 43 (2017) 10299-10306.
[10] H.H. Ussing, P. Kruhoffer, H.J. Thaysen, N. Thorn, The Alkali Metal Ions in Biology: I. The Alkali Metal Ions in Isolated Systems and Tissues. II. The Alkali Metal Ions in the Organism, Springer Science & Business Media2013.
[11] Y. Wang, X. Yang, Z. Gu, H. Qin, L. Li, J. Liu, X. Yu, In vitro study on the degradation of lithium-doped hydroxyapatite for bone tissue engineering scaffold, Materials Science and Engineering: C, 66 (2016) 185-192.
[12] L. Obadia, P. Deniard, B. Alonso, T. Rouillon, S. Jobic, J. Guicheux, M. Julien, D. Massiot, B. Bujoli, J.-M. Bouler, Effect of sodium doping in β-tricalcium phosphate on its structure and properties, Chemistry of materials, 18 (2006) 1425-1433.
[13] L. Obadia, M. Julien, S. Quillard, T. Rouillon, P. Pilet, J. Guicheux, B. Bujoli, J.-M. Bouler, Na-doped β-tricalcium phosphate: physico-chemical and in vitro biological properties, Journal of Materials Science: Materials in Medicine, 22 (2011) 593-600.
[14] A. Cormack, J. Du, T. Zeitler, Sodium ion migration mechanisms in silicate glasses probed by molecular dynamics simulations, Journal of non-crystalline solids, 323 (2003) 147-154.
[15] F. He, C. Ping, Viscosity and structure of lithium sodium borosilicate glasses, Physics Procedia, 48 (2013) 73-80.
[16] C. Huang, A. Cormack, The structure of sodium silicate glass, The Journal of chemical physics, 93 (1990) 8180-8186.
[17] R. Newell, B. Feuston, S.H. Garofalini, The structure of sodium trisilicate glass via molecular dynamics employing three-body potentials, Journal of Materials Research, 4 (1989) 434-439.
[18] T. Uchino, T. Sakka, Y. Ogata, M. Iwasaki, Local structure of sodium aluminosilicate glass: an ab initio molecular orbital study, The Journal of Physical Chemistry, 97 (1993) 9642-9649.
[19] R. Dohmen, S.A. Kasemann, L. Coogan, S. Chakraborty, Diffusion of Li in olivine. Part I: experimental observations and a multi species diffusion model, Geochimica et Cosmochimica Acta, 74 (2010) 274-292.

[20] R. Choudhary, J. Vecstaudza, G. Krishnamurithy, H.R.B. Raghavendran, M.R. Murali, T. Kamarul, S. Swamiappan, J. Locs, In-vitro bioactivity, biocompatibility and dissolution studies of diopside prepared from biowaste by using sol–gel combustion method, Materials Science and Engineering: C, 68 (2016) 89-100.
[21] T. Vela, P. Selvarajan, T. Freeda, K. Balasubramanian, Growth and characterization of pure and semiorganic nonlinear optical Lithium Sulphate admixtured l-alanine crystal, Physica Scripta, 87 (2013) 045801.
[22] I. Nugrahani, S. Asyarie, S.N. Soewandhi, S. Ibrahim, Solid state interaction between amoxicillin trihydrate and potassium Clavulanate, Malays. J. Pharm. Sci, 5 (2007) 45-57.
[23] S. Yang, D. Zhao, H. Zhang, S. Lu, L. Chen, X. Yu, Impact of environmental conditions on the sorption behavior of Pb (II) in Na-bentonite suspensions, Journal of hazardous materials, 183 (2010) 632-640.
[24] F. De Mul, M. Hottenhuis, P. Bouter, J. Greve, J. Arends, J. Ten Bosch, Micro-Raman line broadening in synthetic carbonated hydroxyapatite, Journal of dental research, 65 (1986) 437-440.
[25] S. Koutsopoulos, Synthesis and characterization of hydroxyapatite crystals: a review study on the analytical methods, Journal of Biomedical Materials Research Part A, 62 (2002) 600-612.
[26] R. Vahedifard, E. Salahinejad, Microscopic and spectroscopic evidences for multiple ion-exchange reactions controlling biomineralization of CaO. MgO. 2SiO2 nanoceramics, Ceramics International, 43 (2017) 8502-8508.
[27] E. Salahinejad, R. Vahedifard, Deposition of nanodiopside coatings on metallic biomaterials to stimulate apatite-forming ability, Materials & Design, 123 (2017) 120-127.
[28] H. Takadama, H.-M. Kim, T. Kokubo, T. Nakamura, Mechanism of biomineralization of apatite on a sodium silicate glass: TEM− EDX study in vitro, Chemistry of materials, 13 (2001) 1108-1113.
[29] W. Song, M. Tian, F. Chen, Y. Tian, C. Wan, X. Yu, The study on the degradation and mineralization mechanism of ion-doped calcium polyphosphate in vitro, Journal of Biomedical Materials Research Part B: Applied Biomaterials, 89 (2009) 430-438.
[30] W. Song, Q. Wang, C. Wan, T. Shi, D. Markel, R. Blaiser, W. Ren, A novel alkali metals/strontium co-substituted calcium polyphosphate scaffolds in bone tissue engineering, Journal of Biomedical Materials Research Part B: Applied Biomaterials, 98 (2011) 255-262.
[31] I. Kansal, A. Reddy, F. Muñoz, S.-J. Choi, H.-W. Kim, D.U. Tulyaganov, J.M. Ferreira, Structure, biodegradation behavior and cytotoxicity of alkali-containing alkaline-earth phosphosilicate glasses, Materials Science and Engineering: C, 44 (2014) 159-165.
[32] A. Tilocca, Sodium migration pathways in multicomponent silicate glasses: Car–Parrinello molecular dynamics simulations, The Journal of chemical physics, 133 (2010) 014701.
[33] S. Bose, G. Fielding, S. Tarafder, A. Bandyopadhyay, Understanding of dopant-induced osteogenesis and angiogenesis in calcium phosphate ceramics, Trends in biotechnology, 31 (2013) 594-605.
[34] S. Vahabzadeh, V.K. Hack, S. Bose, Lithium-doped β-tricalcium phosphate: Effects on physical, mechanical and in vitro osteoblast cell–material interactions, Journal of Biomedical Materials Research Part B: Applied Biomaterials, 105 (2017) 391-399.
[35] N.C. Henney, B. Li, C. Elford, P. Reviriego, A.K. Campbell, K.T. Wann, B.A. Evans, A large-conductance (BK) potassium channel subtype affects both growth and mineralization of human osteoblasts, American Journal of Physiology-Cell Physiology, 297 (2009) C1397-C1408.
[36] R. Moreau, R. Aubin, J. Lapointe, D. Lajeunesse, Pharmacological and Biochemical Evidence for the Regulation of Osteocalcin Secretion by Potassium Channels in Human Osteoblast-like MG–63 Cells, Journal of bone and mineral research, 12 (1997) 1984-1992.
[37] L. Liu, P.H. Schlesinger, N.M. Slack, P.A. Friedman, H.C. Blair, High capacity Na+/H+ exchange activity in mineralizing osteoblasts, Journal of cellular physiology, 226 (2011) 1702-1712.

This is the accepted manuscript (postprint) of the following article:
H. Rahmani, E. Salahinejad, *Incorporation of monovalent cations into diopside to improve biomineralization and cytocompatibility*, Ceramics International, 44 (2018) 19200-19206.
https://doi.org/10.1016/j.ceramint.2018.07.140

Figures

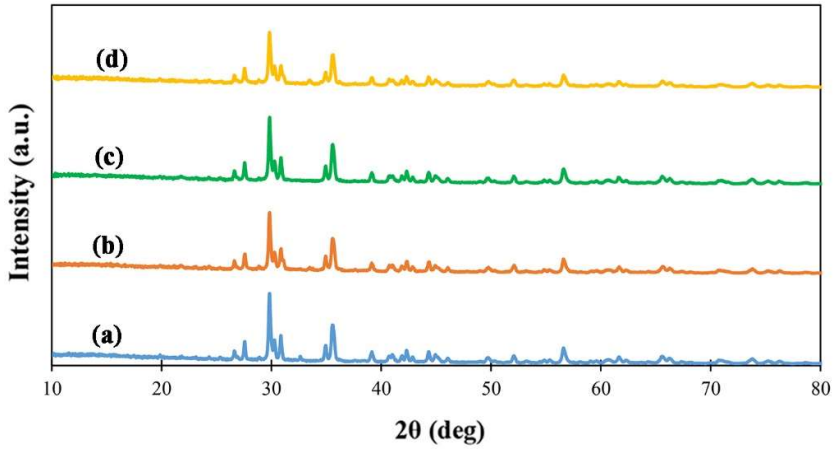

Fig. 1. XRD pattern of the undoped (a), Li- (b), Na- (c), and K- (d) doped samples after calcination. All of the diffraction peaks belong to diopside (Ref. Code: 00-017-0318).

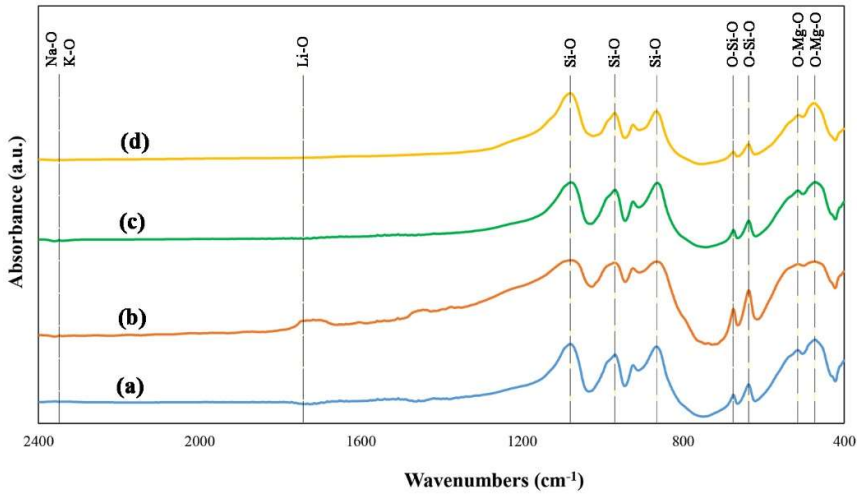

Fig. 2. FTIR spectra of the undoped (a), Li- (b), Na- (c), and K- (d) doped samples after calcination.

This is the accepted manuscript (postprint) of the following article:
H. Rahmani, E. Salahinejad, *Incorporation of monovalent cations into diopside to improve biomineralization and cytocompatibility*, Ceramics International, 44 (2018) 19200-19206.
https://doi.org/10.1016/j.ceramint.2018.07.140

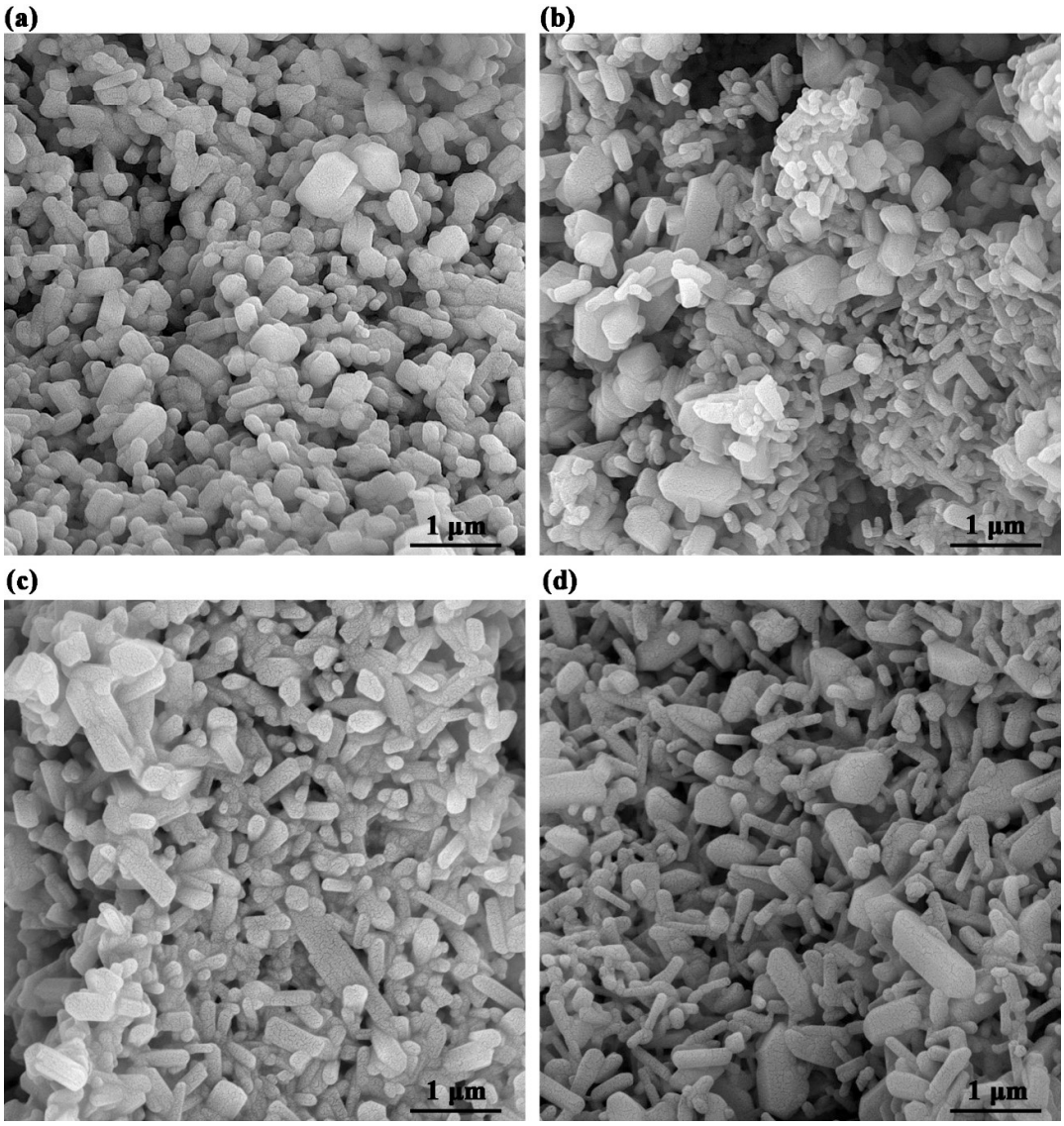

Fig. 3. FESEM micrograph of the undoped (a), Li- (b), Na- (c), and K- (d) doped samples.

This is the accepted manuscript (postprint) of the following article:
H. Rahmani, E. Salahinejad, *Incorporation of monovalent cations into diopside to improve biomineralization and cytocompatibility*, Ceramics International, 44 (2018) 19200-19206.
https://doi.org/10.1016/j.ceramint.2018.07.140

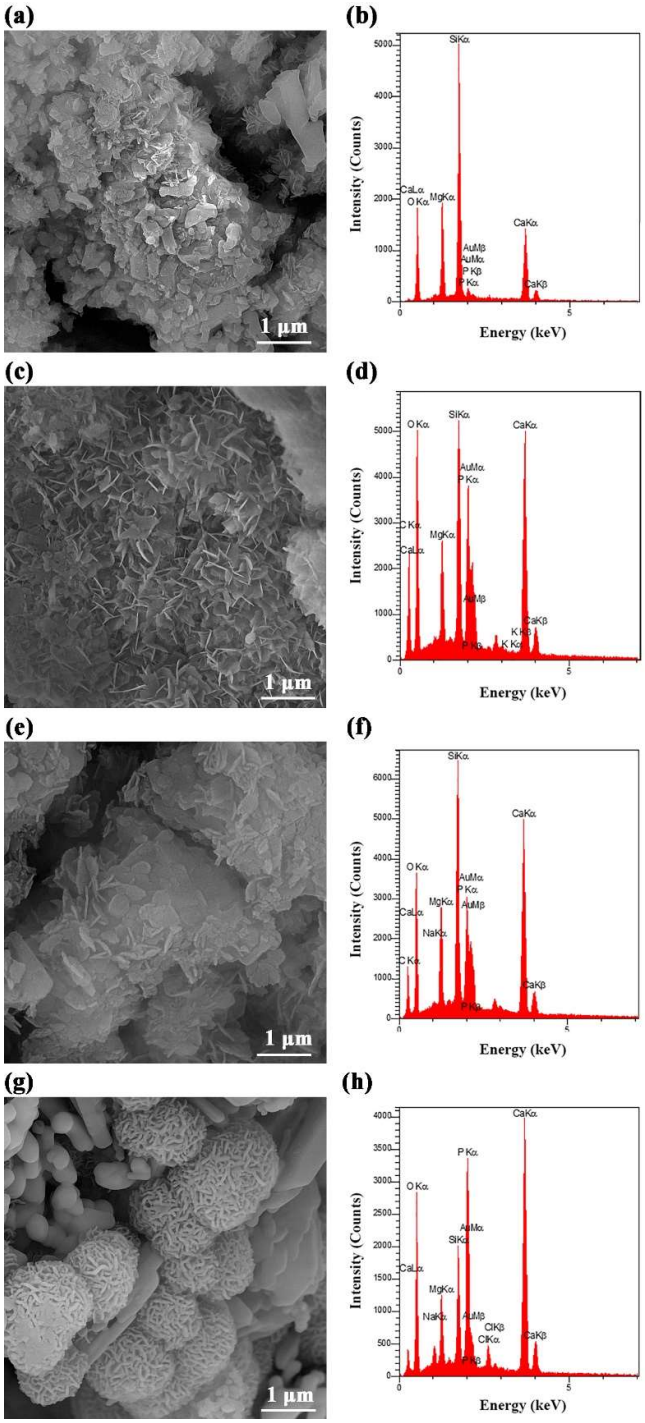

Fig. 4. FESEM micrograph and EDS pattern of the undoped (a, b), Li- (c, d), Na- (e, f), and K- (g, h) doped samples.

This is the accepted manuscript (postprint) of the following article:
H. Rahmani, E. Salahinejad, *Incorporation of monovalent cations into diopside to improve biomineralization and cytocompatibility*, Ceramics International, 44 (2018) 19200-19206.
https://doi.org/10.1016/j.ceramint.2018.07.140

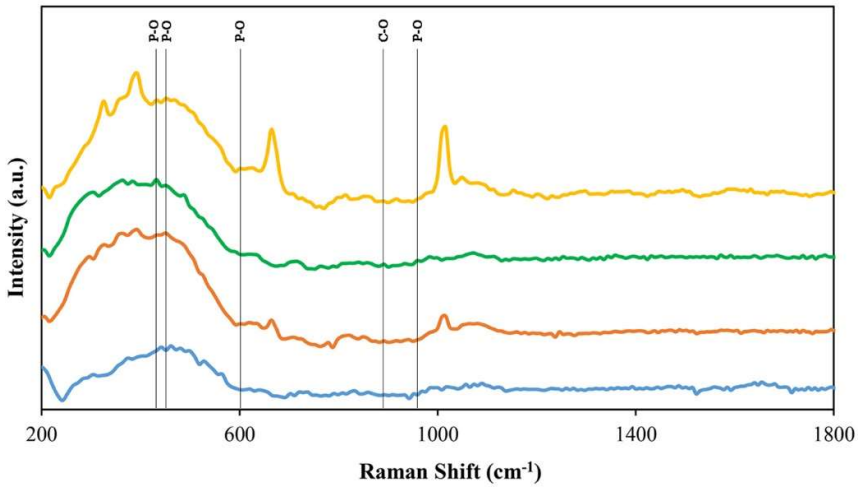

Fig. 5. Raman spectra of the undoped (a), Li- (b), Na- (c), and K- (d) doped samples after immersion in the SBF.

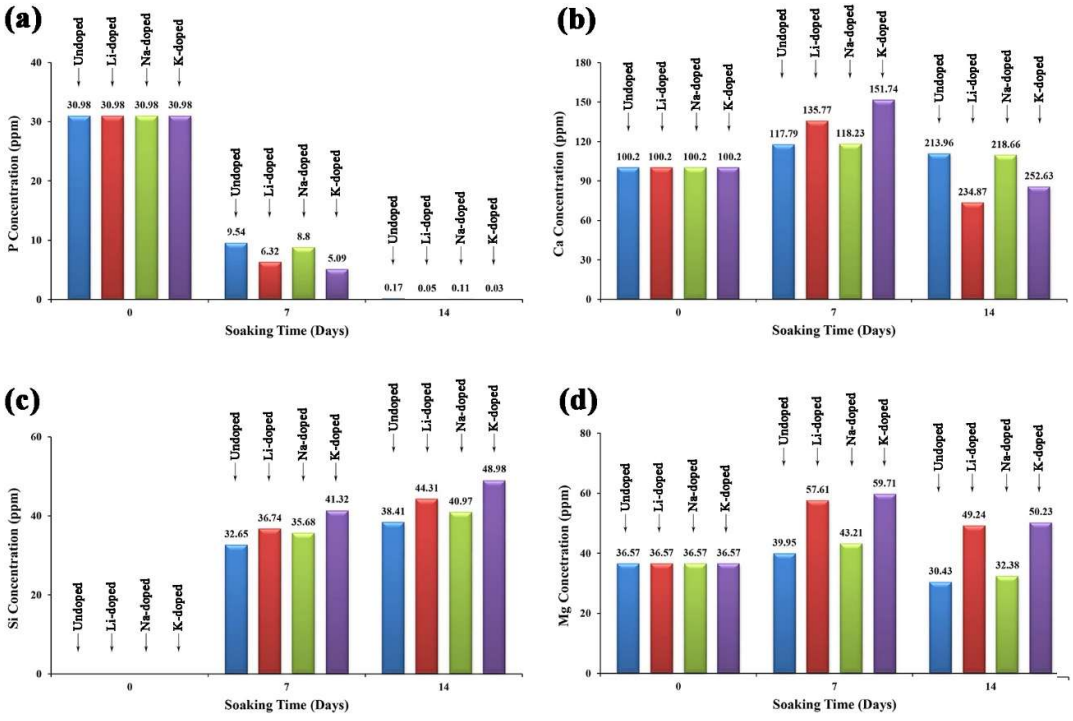

Fig. 6. ICP results of P (a), Ca (b), Si (c), and Mg (d) ions in the SBF.

This is the accepted manuscript (postprint) of the following article:
H. Rahmani, E. Salahinejad, *Incorporation of monovalent cations into diopside to improve biomineralization and cytocompatibility*, Ceramics International, 44 (2018) 19200-19206.
https://doi.org/10.1016/j.ceramint.2018.07.140

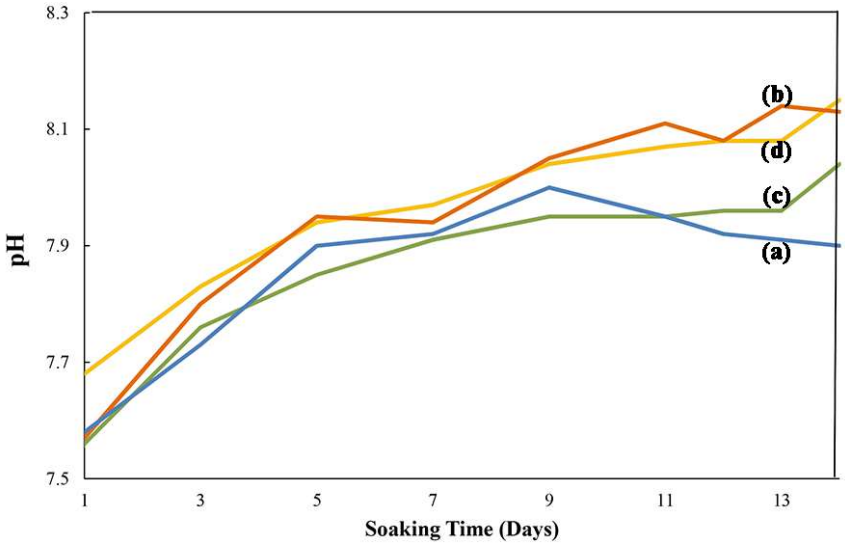

Fig. 7. pH variations of the SBF in contact with the undoped (a), Li- (b), Na- (c), and K- (d) doped samples.

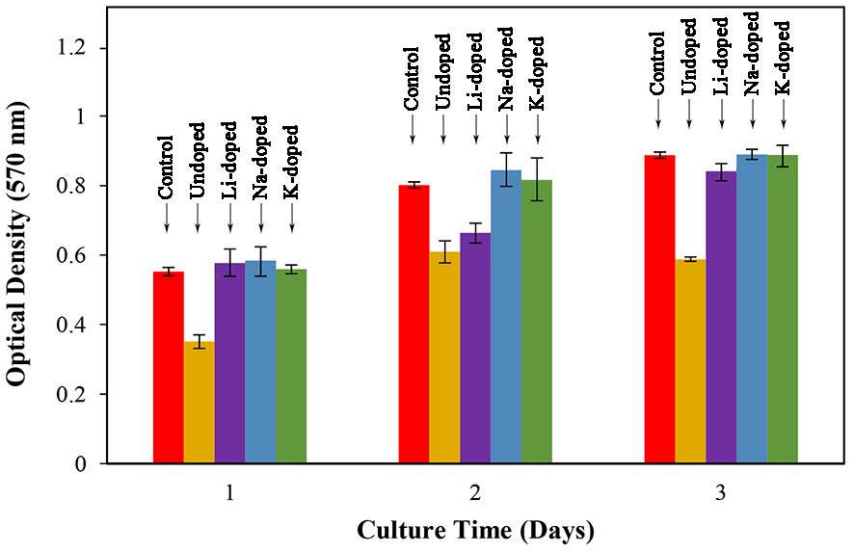

Fig. 8. Results of the MTT assay of the MG-63 cell cultures on the samples.

This is the accepted manuscript (postprint) of the following article:
H. Rahmani, E. Salahinejad, *Incorporation of monovalent cations into diopside to improve biomineralization and cytocompatibility*, Ceramics International, 44 (2018) 19200-19206.
https://doi.org/10.1016/j.ceramint.2018.07.140

Table 1. Crystallographic data of diopside in the different doped structures.

Sample	a (A°)	b (A°)	c (A°)	β (°)	V (Å^3)
Undoped	9.759	8.933	5.265	105.91	441.341
Li-doped	9.752	8.929	5.267	105.98	440.903
Na-doped	9.756	8.933	5.266	105.88	441.391
K-doped	9.760	8.934	5.266	105.83	441.796